Proceedings of ITC18, 2008

3D MHD equilibrium calculations for Tokamaks with resonant magnetic perturbations: TEXTOR as an example

Christopher WIEGMANN[1)], Yasuhiro SUZUKI[2)], Joachim GEIGER[3)], Yunfeng LIANG[1)], Detlev REITER[1)], Robert C. WOLF[3)]

[1)]*Institut für Energieforschung - Plasmaphysik, Forschungszentrum Jülich GmbH, Assoziation EURATOM-FZJ, Trilateral Euregio Cluster, 52425 Jülich, Germany*

[2)]*National Institute for Fusion Science, 322-6 Oroshi-cho, Toki 509-5292, Japan*

[3)]*Max-Planck-Institut für Plasmaphysik, Assoziation EURATOM-IPP, 17491 Greifswald, Germany*

For the first time three dimensional equilibrium calculations for the tokamak TEXTOR with dynamic ergodic divertor are presented. These calculations were performed with the HINT2 code which was applied for the first time to tokamaks with high net toroidal current and island structures. The results are compared with the often used vacuum superposition approach. In case of the DED in 6/2 mode the differences are found to be minor. In case of the DED in 3/1 mode, a large appearing 1/1 island in the core plasma shows that a further understanding of the treatment of the net toroidal current density has to be achieved.

Keywords: MHD equilibrium, TEXTOR, DED, HINT2

1 Introduction

The application of **R**esonant **M**agnetic **P**erturbations (RMP) to tokamaks recently gained a lot of attention due to the possibility of ELM suppression or mitigation [1, 2]. The iron core tokamak TEXTOR with circular plasma cross-section is specially suited to study the 3D effects of RMPs due to its **D**ynamic **E**rgodic **D**ivertor (DED) [3]. The DED consists of 16 helically aligned perturbation coils installed in-vessel at the high-field side and can be operated in several base modes (m/n = 12/4, 6/2 and 3/1) with either DC or AC current supply. The penetration depth of the RMPs depends on the choosen poloidal mode number m.
Knowledge of the magnetic field topology is a necessary prerequisite for further studies concerning e.g. the transport charateristics. Earlier work on error field penetration has shown strong indications that screening and amplification of RMPs play an important role in determining the magnetic field topology (see e.g. [4, 5]). Nevertheless, in this study a full penetration of the RMPs is assumed. The focus lies on the effect of the RMPs on the plasma equilibrium itself as the equilibrium force balance is distorted. The converged 3D equilibria will be compared with the simple vacuum assumption.

2 HINT2 code

To investigate the resulting 3D equilibrium the HINT2 code [6, 7] is applied. This code is an Eulerian initial value solver which relaxes the given initial magnetic field configuration into an equilibrium by solving resistive MHD equations. Screening of the RMPs due to plasma rotation is not taken into account.
HINT2 uses a quasi-eulerian helically rotating grid (u^1, u^2, u^3) which in case of tokamak calculations reduces to a cylindrical like coordinate system whose relation to normal cylindrical coordinates is given by

$$r = R_0 + u^1 \tag{1}$$

$$z = u^2 \tag{2}$$

$$\phi = -u^3 \,. \tag{3}$$

The relaxation process is carried out in two steps. Instead of solving the evolution equation for the pressure, the pressure distribution is relaxated in step A with fixed magnetic field by a field line tracing method. The pressure is adjusted to satisfy a vanishing pressure gradient along the field lines ($\mathbf{B}\cdot\nabla p = 0$) by evaluating the line integral along a field line

$$p^{i+1} = \bar{p} = \frac{\int_{-L_{in}}^{L_{in}} F p^i \frac{dl}{B}}{\int_{-L_{in}}^{L_{in}} \frac{dl}{B}}, \quad F = \begin{cases} 1 & : \text{ if } L_C \geq L_{in} \\ 0 & : \text{ if } L_C < L_{in} \,. \end{cases} \tag{4}$$

On field lines which leave the computational region or intersect with a limiting contour the pressure is set to zero. Depending on the value of L_{in} a finite pressure in the stochastic edge region can be sustained. Hence, L_{in} plays a crucial role in describing the vacuum-plasma transistion.
In step B, a set of resistive MHD equations with fixed pres-

author's e-mail: c.wiegmann@fz-juelich.de

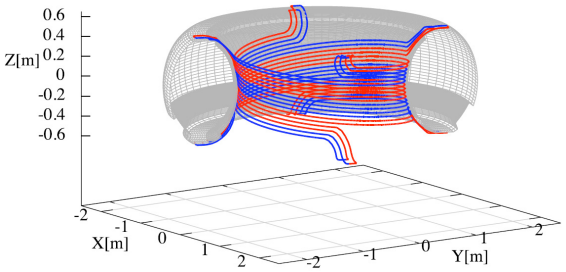

Fig. 1 DED in 6/2 configuration with the limiting contour used in HINT2 calculation.

sure distribution is solved

$$\frac{\partial \mathbf{v}}{\partial t} = -f_{CFL}\left(\nabla p + (\mathbf{J} - \mathbf{J_0}) \times \mathbf{B}\right) \quad (5)$$

$$\frac{\partial \mathbf{B}}{\partial t} = \nabla \times \left\{ \mathbf{v} \times \mathbf{B} - \eta \left(\mathbf{J} - \mathbf{J_0} - \mathbf{B} \frac{\langle \mathbf{J} \cdot \mathbf{B} \rangle_{net}}{\langle B^2 \rangle} \right) \right\} \quad (6)$$

$$\mathbf{J} = \nabla \times \mathbf{B}, \quad \mathbf{J_0} = \nabla \times \mathbf{B_{vac}}. \quad (7)$$

The factor f_{CFL} is necessary to ensure that the Courant-Friedrich-Levy condition is satiesfied in case that field coils are located inside the computational domain. $\mathbf{J_0}$ denotes the vacuum current density due to the poloidal and toroidal coils within the computational domain. The net toroidal current density $\mathbf{B}\frac{\langle \mathbf{J}\cdot\mathbf{B}\rangle_{net}}{\langle B^2\rangle}$ is made up by the ohmic current, the bootsstrap current, currents due to heating and current drive schemes. A functional dependence on the normalized toroidal flux is assumed.

3 Calculation results

The input data for the HINT2 calculation were prepared as follows. Usually, a 3D free boundary equilibrium calculation assuming nested flux surfaces, typically done with the VMEC code [8,9], is used to initialize the HINT2 calculations. In case of TEXTOR, this procedure is not applicable due to the existing iron core and a missing 3D model taking the iron core effects into account. Instead, a version of the 2D equilibrium code DIVA, specially adapted for TEXTOR and the iron core, is used to provide an axisymmetric 2D equilibrium. The perturbation field of the DED is calculated via Biot-Savart from the given polygon description which also includes the current feeds (see Fig.1). The initial total magnetic field for HINT2 is than a superposition of the 2D equilibrium, an $1/R$ toroidal field corrected for the diamagnetic behaviour of the plasma and the vacuum perturbation field. To obtain an initial 3D pressure distribution, the calculated 2D pressure of DIVA is mapped toroidally. The net toroidal current density profile is obtained by surface averaging the toroidal current density profile of DIVA and mapping this with the help of the safety factor profile onto the normalized toroidal flux.
As the DED coils are located very close to the plasma itself, the usage of a limiting contour in the calculation is inevitable. Otherwise, stochastic field lines extending from the plasma into the coil region could be captured there and could lead to an additional build up of a finite pressure in the plasma edge region as their connection length exceed L_{in}.

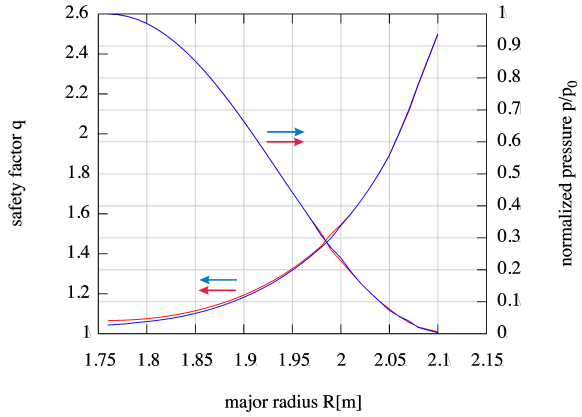

Fig. 2 Pressure and safety factor profiles of vacuum superposition (red) and 3D equilibrium (blue) of DED in 6/2 configuration, both at the toroidal angle $\phi = 0$.

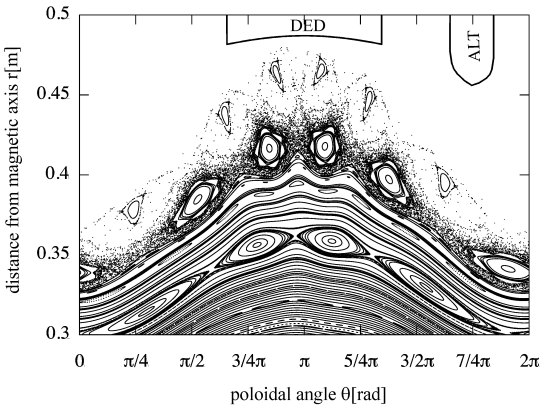

Fig. 3 Edge region of the 3D converged equilibrium for the DED 6/2 case at $\phi = 0$. At the top, the limiting structures of the DED (middle) and of the ALT-limiter (upper right) can be seen. The 4/2 island chain inside the core plasma and the remanent 5/2 and 6/2 island chains are clearly visible.

3.1 TEXTOR with DED 6/2

Here, a 3D equilibrium for TEXTOR with a DED 6/2 perturbation field was calculated. Due to the perturbation field symmetry only a half torus calculation was necessary. The resolution was chosen to be $129 \times 129 \times 184$ grid points (u^1, u^2, u^3) corresponding to a spacial resolution of $1.02cm$ in a poloidal plane and about $1°$ in toroidal direction. The underlying 2D equilibrium had the following parameters: $I_p = 245kA$, $B_{tor}(@1.75) = 1.3T$ and a central axis pressure of $p_{axis} = 16kPa$.
In step A, $L_{in} = 200m$ was used for the pressure relax-

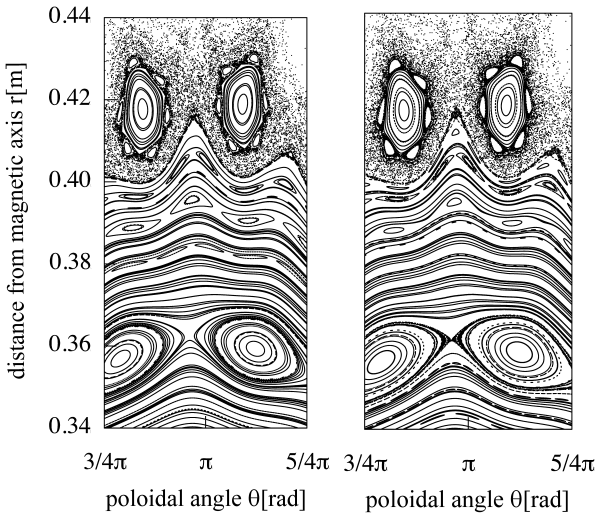

Fig. 4 Enlarged area of vacuum superposition (left) and converged 3D equilibrium (right) for the DED 6/2 case.

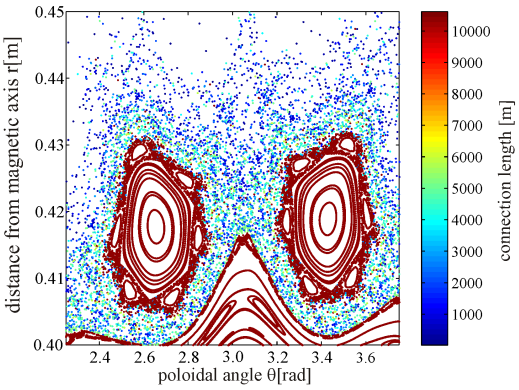

Fig. 5 Connection length plot of enlarged area of vacuum superposition of DED in 6/2 configuration at $\phi = 0$.

ation to ensure that the inner islands are traced out completely and the pressure profile is flattened there accordingly. In Fig.2 the profiles for the safety factor q and the pressure p as functions of the major radius are shown for the vacuum superposition and the converged 3D equilibrium. Both profiles do not differ very much from each other. Deviations in the pressure profiles can especially be seen in the plasma edge and can be assigned to the location of the islands and stochastic region. The q-profiles agree well in the edge region but the 3D equilibrium one has a slightly lower value in the core region. This is caused by the changed net toroidal current distribution. Furthermore, the q-profiles can only be computed up to a major radius of $2.1m$ as it is not possible to compute a q-value further out due to the ergodicity of the edge region. The Differences around $r_{minor} = 1.98 - 2.0m$ are due to the $3/2$ island chain.

The magnetic field structure of the converged equilibrium is shown in Fig.3 for the edge region. The gross structures agree very well between the vacuum superposition and the 3D equilibrium. This can be attributed to the

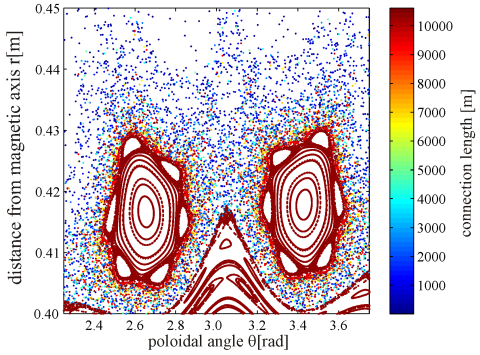

Fig. 6 Connection length plot of enlarged area of converged 3D equilibrium of DED in 6/2 configuration at $\phi = 0$.

low plasma pressure and current in the edge region resulting in a very small modification of the magnetic topology due to the equilibrium response. Having a closer look, a starting ergodisation of the X-point of the $4/2$ island chain at $r \approx 0.36m$ can be observed in the converged equilibrium case (see Fig.4). Furthermore, the island width of the high m island chain at $r \approx 0.39m$ has decreased. Connection length plots for both cases are shown for an enlarged area in Fig.5 and Fig.6, respectively. In both cases a sharp separation between the stochastic region and the remanent $5/2$ islands as well as the core area can clearly be seen. But in case of the converged 3D equilibrium the separation between the remanent $5/2$ islands and the surrounding stochastic region is no longer that pronounced as it is in the vacuum superposition case.

3.2 TEXTOR with DED 3/1

As the perturbation field of the DED 3/1 configuration offers no symmetry, a full torus calculation is necessary. The resolution was chosen to be $121 \times 121 \times 184$ resulting in a spacial resolution of exactly $1.0cm$ in a poloidal plane. The toroidal resolution had to be decreased to 2° due to computational costs, especially memory needs. As underlying 2D equilibrium the following parameters were choosen: $I_p = 300kA$, $B_{tor}(@1.75m) = 2.25T$ and an axis pressure of $p_{axis} = 8.6kPa$. As TEXTOR discharges tend to be sawtooth unstable in this scenario, an axis value of the safety factor below one was chosen for the underlying DIVA equilibrium. Consequently, by adding the DED field a large $1/1$ island appears. The vacuum superposition and the converged equilibrium solution are shown in Fig.7 and Fig.8, respectively. The $1/1$, $2/1$, $3/1$ and $4/1$ islands are clearly visible. Major changes in the magnetic field topology can be observed around the magnetic axis and the $1/1$ island in the converged equilibrium case. A closer analysis shows then that these changes are not caused alone by physics but that the pressure profile is not flattened accordingly within the $1/1$ island evenso the value of L_{in} was choosen sufficiently high. An accurate

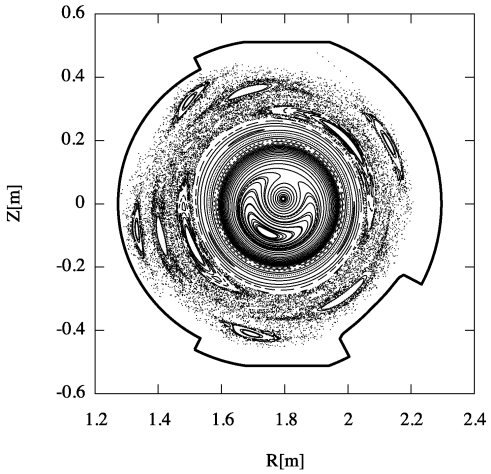

Fig. 7 Vacuum superposition of the DED in 3/1 configuration and 2D equilibrium at $\phi = 0$.

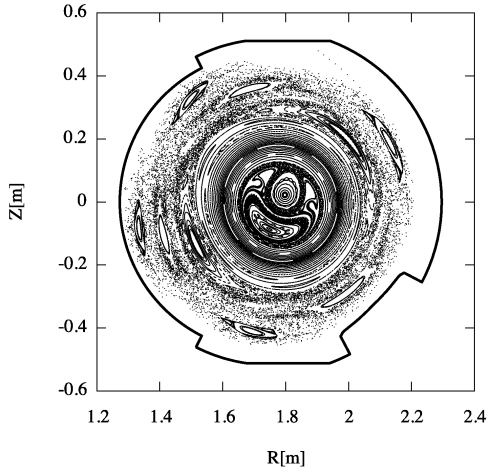

Fig. 8 Converged 3D equilibrium of the DED in 3/1 configuration at $\phi = 0$.

flattening is a necessity in case of tokamak calculations with the HINT2 code as the toroidal flux distribution is calculated from the relaxated pressure distribution and than used for distributing the net toroidal current density. Here, a small deepening of the pressure profile within the 1/1 island leads to a deepening of the calculated toroidal flux distribution and then to a wrong scaling of the net toroidal current. This causes a net toroidal current distribution, which compromises island confinement, as shown in Fig.9, and drives then via Eq.(6) the modification of the magnetic field topology, which in this case is partly caused by numerics.

4 Conclusions

The presented DED 6/2 case shows only very minor changes in the converged equilibrium solution so that the vacuum superposition appears to be a resonable approxi-

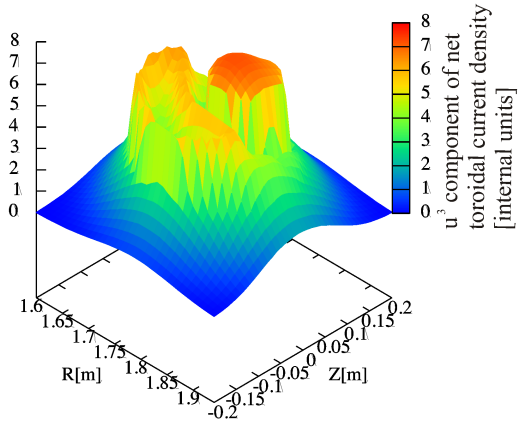

Fig. 9 Surface plot of the net toroidal current density [internal units] in the plasma core region of the converged 3D equilibrium of the DED in 3/1 configuration at $\phi = 0$.

mation for the considered case. The low equilibrium response can be attributed to the low pressure gradient and current density in the edge. Furthermore, the chosen parameter $L_{in} = 200m$ leads to a smoothed pressure distribution in the ergodic edge region. Lower values of L_{in} could give a better resemblance of the local pressure distribution and could lead to a higher pressure in the edge region but will cause an insufficient profile flattening of the core islands. The effect of different values for L_{in} will be studied in the future.

For the 3/1 configuration, the picture is different. Here, a large 1/1 island in the core plasma causes numerical problems in the distribution of the net toroidal current density due to an inaccurate normalized toroidal flux distribution. For studying the 3/1 configuration with safety factor profiles, whose value is below one at the axis, or tokamak equilibria with large internal islands an improvement of the pressure flattening algorithm or of the calculation of the flux distribution will be necessary. Furthermore, the grid dependence of these effect has to be studied.

Acknowledgements One of the authors (C.W.) gratefully acknowledges support by a "Pre/Postdoctoral Scholarship for North-American and European Researchers (Short Term)" of the Japan Society for the Promotion of Science (JSPS).

[1] Y.Liang et al., Phys. Rev. Lett. **98**,265004 (2007).
[2] T.E. Evans et al., Nature Phys. **2**, 419 (2006)
[3] K.H. Finken et al., *The structure of magnetic field in the TEXTOR-DED*, Schriften des Forschungszentrum Jülich, Energy Technology **45**, ISSN 1433-5522 (2005)
[4] Q. Yu et al., Nucl. Fusion **48**, 024007 (2008)
[5] Y. Kikuchi et al., Plasma Phys. Control. Fusion **48**, 169-183 (2006)
[6] Y. Suzuki et al., Nucl. Fusion **46**, L19-L24 (2006)
[7] K. Harafuji et al., J. Comp. Phys. **81**, 169-192 (1989)
[8] S.P. Hirshman and D.K. Lee, Comput. Phys. Commun. **43**, 143 (1986)
[9] S.P. Hirshman et al., Comput. Phys. Commun. **43** (1986)